CHARACTERIZATION OF CELLULOSE NANOCRYSTALS FROM A PILOT SCALE FACILITY: THE EFFECT OF A PRETREATMENT STAGE AND DIFFERENT DRYING METHODS

MICHAEL GEORGE, WEI-ZHENG SHEN, KUMAKSHI SHARMA and CARLO MONTEMAGNO

Department of Chemical and Materials Engineering, University of Alberta, Edmonton, Alberta T6G 2M9, Canada
✉ *Corresponding author: C. Montemagno, montemag@ualberta.ca*

Received July 19, 2016

Cellulose nanocrystals (CNCs) are obtained as slurry, which needs to be dried for storage and transport. In this paper, the effect of drying CNCs at a pilot scale facility and caustic pretreatment of the starting material on the final properties of the CNCs is investigated. Surface characterization confirmed drying does not impact the chemical signatures, abundance of fragments, and polarity, based on infrared, secondary ion mass spectroscopy, and contact angle measurements, respectively. Also, the particle distribution, charge, and thermal properties were unaffected. These results were confirmed when compared to those reported by National Research Council of Canada, when they analyzed the properties of a standard CNC material. Also, it was found that caustic pretreatment does not influence the final properties of the CNC particles produced. Nevertheless, based on observations made from scanning electron micrographs, agglomeration was the key drawback when drying CNCs.

Keywords: cellulose nanocrystals, drying, surface characterization, thermal characterization

INTRODUCTION

Cellulose is the most abundant renewable natural polymer found on earth. It is estimated that cellulose is produced at an annual rate of 50 billion metric tons.[1] In fact, cellulose constitutes 40-60 wt% of dry wood and accounts for more than 70% of most natural fibres. In plants, cellulose is synthesized as structural microfibrils in the cell walls with different microfibrillar arrangements. Specifically, a random network of individual elements form in the primary cell wall, while an ordered or layer-like structure builds up in the secondary cell walls. Cellulose microfibrils have diameters between 2 and 200 nm and lengths varying from several microns, depending on the origin.[1]

Cellulose nanocrystals (CNCs) are obtained by strong acid hydrolysis or oxidation of cellulose crystals from cellulose microfibrils in forest products, residues, or other sources.[2-3] CNCs have created a paradigm shift in many areas in the past decade because they are biocompatible, biodegradable, and can be obtained from a variety of natural and renewable sources. Furthermore, the chemical, physical, and mechanical properties of CNCs make it a potential material to replace many petrochemical-based platforms.[4-5]

At the moment, several agencies and companies in Canada have pioneered large-scale pilot production of CNC. FPInnovations (Quebec), CelluForce (Quebec), Alberta Innovates Technology Futures (Alberta), and BlueGoose Biorefineries (Saskatoon – private company) are some of the major ventures that come to mind when considering Canada. Also, the U.S. Forest Service, in collaboration with the U.S. National Nanotechnology Initiative, recently held a workshop geared towards realizing the prospect of commercializing CNC production in the U.S.

According to TAPPI Nanotechnology for Renewable Nanomaterials Conference (TAPPI Nano Atlanta-June, 2015) CelluForce (Canada), American Process (USA), Holmen (Sweden), and Alberta Innovates Technology Futures (Canada) are the main producers of CNCs on a large scale (output > 20 kg/day) across the globe. Nevertheless, smaller producers (output < 10 kg/day) include US Forest Products Lab, BlueGoose Bio. (Canada), India Council for

Agriculture Research (India), FPInnovations (Canada), and Melodea (Israel). Finally, the production of CNCs has been constantly researched and output capacities are increasing.

In a paper published by Shatkin[6] *et al*. outlining the market projection of cellulose nanomaterial enabled products, the authors reported estimates of the market volume on the basis of estimate tonnage of cellulose nanomaterial production rather than the dollar value or profits from production. At the moment, the U.S. market potential for identified applications of nanocellulose is estimated at 6.4 million metric tons, with a global market potential of 35 million metric tons. Further, the greatest application for nanocellulose has been the paper and packaging industries. Other potential high-value and high-volume uses are in the automotive, construction, personal care, and textile sectors.[6]

CNCs have high specific surface area and energy. As a result, they aggregate and form larger particles during the drying phase of processing. A few key applications can use CNCs as a suspension, including biocomposite and bioplastic applications. However, in an effort to reduce transportation costs and suitability for other applications, such as biomedical scaffolds and drilling applications, the material needs to be dried. Hence, CNCs particles have been freeze-dried[7] and spray dried[8] for these applications. In the freeze drying method or lyophilization, low temperature (by sublimation) is employed to blast the water molecules out of the samples. It is especially suitable for thermo-sensitive materials. On the other hand, for spray drying, the suspension is atomized inside a drying chamber where hot air (> 105 °C) is used as the drying atmosphere. Both of these drying methods are believed to have significant influence on the final properties of the CNCs.

In this work, the effect of spray drying or freeze-drying on the chemical signatures, thermal, and morphological features of CNCs obtained from a pilot scale facility are reported. Also, the effect of pretreating the feedstock (softwood pulp) with a caustic treatment to produce a regenerated sample is reported. It is of utmost importance to characterize samples from the pilot plant to ensure the properties measure up to those produced at the lab scale. These samples were characterized along with a standard CNC sample provided by the National Research Council of Canada and Alberta Innovates Technology Futures. A comprehensive suite of techniques was used to investigate the influence of drying and pretreating the material. This is one of the first studies to outline a comprehensive report on CNC properties and implications to industry.

EXPERIMENTAL

Materials

Samples of cellulose nanocrystals (CNC) were obtained from a pilot scale facility located at Alberta Innovates Technology Futures, Edmonton, Canada. The different samples were stored at room temperature until characterization. A summary of the feedstock, methods used for drying the samples, and treatment carried out is given here. The CNC samples (freeze-dried, spray dried, and regenerated) were obtained *via* hydrolysis of dissolving pulp. Reaction parameters of 120 minutes, 45 °C, stirring at 200 rpm, and a sulfuric acid concentration of 64 wt% were used to produce the samples. An acid:pulp consistency of 12:1 was used for all experiments. The regenerated sample was obtained by treating the dissolving pulp with 5% (w/w) caustic for 60 minutes prior to acid treatment. National Research Council of Canada provided this material in kind. In extension, this material was supplied by FPInnovations (Pointe-Claire, Quebec) to NRC. The material was extracted using sulfuric acid hydrolysis of bleached Canadian softwood kraft pulp. The CNC suspension obtained was then spray dried to yield a powder, which was then homogenized by rolling in a clean bottle for 24 hours. In the present paper, the properties of this standard material as reported by NRC will be presented alongside that processed in this study.

Methods

Preparation of CNC

The standard protocol for production of CNC is outlined above (reaction parameters are outlined in "Materials" section). CNC was produced *via* acid hydrolysis of the softwood pulp supplied to the pilot plant. The pulp and acid were added to the reactor, which was constantly agitated and heated. Upon completion of the hydrolysis, the slurry was pumped into a holding tank, where it was diluted and neutralized. The next phase of production involved separation of the high-value CNC from impurities. The first stage involved using centrifugation to settle out impurities. The next phase involved a series of tangential flow filtration units that separated any final impurities and concentrated the CNC material into a final holding tank, for drying. In the end, the efficiency of the process relies on the final sample clean-up and drying. Hence, it is very important to understand how the properties of the material are altered because of this final stage. The standard and regenerated samples were spray dried before all analyses.

Surface characterization of CNC samples

Contact angle/powder wettability

The powder wettability of the different CNC samples was evaluated using an optimized method developed by George[9] *et al.* for compact powders. In these experiments, a 700 Sigma OneAttension tensiometer was used to measure the change in mass with time when the sample was slowly lowered into a container with distilled water. In brief, the powdered CNC samples were compacted into a glass vessel fitted with a fine sinter glass porous bottom, which allowed for the liquid (distilled water) to penetrate, but preventing the powder from falling through. In effect, when the bottom of the vessel touches the liquid surface, the liquid penetrates, and absorbs into the powder, resulting in uniform wetting of the powder material. A complimentary software supplied with the tensiometer recorded the changes in mass as a function of time.

Prior to sample analysis, samples were pre-conditioned at 50 °C for 4 hours. Triplicate analysis was done for each CNC type. The contact angle of the different samples was evaluated based on the assumptions and equations provided. The main theory is that when a porous solid is in contact with a liquid whereby the solid is not submerged in the liquid, but just touching the liquid's surface, then the rise of liquid into the pores of the solid due to capillary action is given by the following equations (George *et al.*):[9]

$$t = Am^2 \quad (1)$$

where *t* is time after contact, m is the mass of liquid absorbed into the solid, and A is a constant, which is dependent on the properties of the liquid and the solid in question.

Also

$$A = \frac{n}{c\,\rho^2 \sigma \cos\theta} \quad (2)$$

where ç is viscosity of liquid, c is material constant characteristic of solid sample, ñ is density of liquid, ó is surface tension of liquid, and è is contact angle. Equating Equations 1 and 2, we obtain:

$$\cos\theta = \frac{m^2}{t}\,\frac{n}{\rho^2\,\sigma\,c} \quad (3)$$

Given that the viscosity (8.94×10^{-4} Pa/s), density (0.999 g/mL), and surface tension (72.8 dynes/cm at 20 °C) of water are known and the mass of the liquid that rose into the solid was monitored as a function of time (t), only two unknowns are left, contact angle and material constant for the solid. In order to account for this, an experiment was done with hexane. Hexane was chosen because hypothetically it has a contact angle of zero.

Finally, the contact angle of the different CNC powders was evaluated using the method outlined.

Carbon signatures, O/C and [S]

X-ray photoelectron spectroscopy measurements were performed with a Kratos Ultra 165 X-ray Photoelectron Spectrometer with energy spectra ranging from 0-1000 eV. Samples were scanned for C1s (284 eV) and O1s (530 eV). The low-resolution survey scans were taken with a 50 eV step and 160 eV analyzer pass energy. For each sample, the CNC samples were placed on aluminum foils and compressed between the nickel plates. The entire sample assembly (4 total samples) was then placed in the sample chamber for subsequent analysis. In these specific instances, an eight-channel multi-detector was employed for analysis.

All raw data obtained were processed using CasaXPS software (Casa Software Ltd., UK), provided by the home laboratory (nanoFab – University of Alberta). In the end, the mole fractions were estimated using normalized peaks based on acquisition parameters after a linear background subtraction, and consideration of experimental sensitivity factors. C1s spectra were analyzed with a Gaussian product function, by maintaining the full width half maximums (FWHMs) of all components within the range of 1.200 to 1.600.[9-10]

The XPS data provided an idea of the abundance of the different C1s signatures that comprise the different CNC samples and the quantity of O1s within the samples. These measures serve to give an indication of the different C functionality on the surfaces of the particles and the relative hydrophilicity of the CNC samples, respectively.

Fragments on the surface

Secondary ion mass spectroscopy was used to determine the fragmentation pattern of the chemical constituents on the CNC sample surfaces when sputtered with fast ions. A ToF SIMS IV (Ion ToF GmbH) instrument equipped with a reflectron ToF analyzer was used to evaluate all CNC samples. A method previously reported by George[9] *et al.* was closely followed for instrument set-up and sample preparation. Prior to sample analysis, all samples were conditioned in an oven at 50 °C for 5 hours. The primary ion beam used was a 20 keV $^{69}Ga^+$ ion beam rastered over a sample analysis area of 0.5 mm by 0.5 mm covered with CNC particles at a rate of 5 kHz. The beam current used was constantly maintained at approximately 0.4-0.6 nA and the pulse width 25-30 nm, which resulted in primary ion dose within the static SIMS regime. An operating pressure of 10^{-9} mbar was maintained during all sample analysis. Mass range of 0-200 m/z was presented for all samples.

FTIR characterization

CNC samples were analyzed using a Nicolet 8700 FT-IR Spectrometer. FTIR spectra were measured from 400 to 4000 cm^{-1} at a resolution of 4 cm^{-1}. Approximately 0.01 g of the dried sample was pressed into a flat pellet using an ICL 1 ton pellet press. A fixed ratio of KBr to sample (300:1 mg) was maintained for all samples. Each sample was analyzed

at least three times and for each run; 32 scans were made.

Morphological characterization

Micrographs of the CNC surfaces were taken using a Zeiss Sigma Field Emission Scanning Electron Microscopy (FE SEM) equipped with an Everhart-Thornley Secondary Electron Detector (ET-SE), equipped with a state of the art Gemini column for maximum resolution at 1.5 nm at 20 kV accelerating voltage. A gold sputter coater was used to induce conductivity for all samples. A resolution of 4 nm was used for all samples. Approximately 0.1 mg of sample was mounted on conductive adhesive tape, sputter-coated and observed using a voltage of 15-20 kV. The main aim was not to re-disperse the CNCs in solution, but to investigate the morphological changes caused by the drying process.

Bulk properties of different CNC samples

Wide-angle X-ray scattering (WAXS)

All experiments were carried out on a Bruker-AXS, D8 Discover diffractometer system equipped with a Vantec-500 area detector and Cu $K\alpha_1$ radiation source (λ = 1.542 A). The instrument was operated at 40 kV and 30 mA for X-ray diffraction (XRD) experiments. The XRD patterns were obtained by irradiating the film from phi = 00 ~ -180^o over the angular range of 2θ = 5 ~ 80^o for 300 seconds.

XRD patterns of the CNC in the in-plane helped visualization of the distribution of the alignment. The azimuthal profiles of the equatorial reflection (200) allowed quantification of the CNC orientations.[11] The degree of orientation (Π) was calculated according to Equation 4, where FWHM is the full width at half-maximum:

$$\Pi = \frac{180 - FWHM}{180} \quad (4)$$

The peak deconvolution method was used to distinguish the CNC peaks in XRD spectra, as previously reported by Hamad and Hu (2010). In brief, the individual crystalline peaks were extracted from the diffraction intensity profiles by a curve-fitting process. A peak-fitting program (Fityk 0.9.8; http://fityk.nieto.pl/) was used, assuming Gaussian functions for each peak and a broad peak at around 21.5° assigned to the amorphous contribution. Iterations were repeated until the maximum F-number was obtained. In all cases, the F-number was >10,000, which corresponds to an R^2 value of 0.997.[12]

The curve fitting procedure required assumptions about the shape and number of peaks. CNC's diffraction peaks were assigned to 2θ = 16.5, 22.5, 34.6, which are characteristic of planes 110, 200, and 400.[13-15]

After deconvolution of the spectrum, the crystallinity was calculated as the ratio of the area of all crystalline peaks to the total area.

Dynamic light scattering (DLS)

DLS (Zetasizer, Malvern Instruments, UK) was employed to determine the hydrodynamic radii of the nanoparticles from the different samples. The CNC samples were redispersed to around 2 wt% in water, and then sonicated to ensure good dispersion. The resulting mixture was then diluted to 0.1 wt% in DI water. The 0.1% (wt) dispersion was then diluted to a 1:1 ratio using 10 mM NaCl to obtain 0.05% (wt) CNC dispersion in 5 mM NaCl. The suspension was subsequently filtered through a 0.45 µm syringe filter. Measurements were taken using 1 mL of each sample, done in triplicate.

Thermal gravimetric analysis

The effect of different drying methods and of the sample clean-up process was studied using TGA. Samples were tested using a Thermal Analysis Instruments TGA Q50 (TA Instruments) apparatus under a flow of nitrogen to study the effects of heating on the stability of the different treated natural fibres. Platinum pans were used given the high temperatures and the ease of cleaning. The temperature range selected was from room temperature to 600 °C at a rate of 10 °C increase per minute. Triplicate runs were done for each level per treatment. All results were reproduced with 5% error or better.

Statistical analysis

Statistical analyses were done as previously outlined by George *et al*.[10] Each treatment was done in triplicates and results are reported as the mean ± standard deviation. All statistical analyses of the raw data were conducted using the statistical software package SAS Version 9.4. For most samples, t-test was used to determine significance. In cases with non-parametric data, the Kruskal Wallis Test was applied to the data populations involved, with a 95% confidence level ($p < 0.05$).

RESULTS AND DISCUSSION

Surface characterization of cellulose nanocrystals

Contact angle measurements

The contact angles of the different samples were evaluated using a Biolin Scientific instrument calibrated for measuring the wettability of powders. The results are presented in Table 1. As can be observed, the CNC samples were characterized with the contact angle between 39-43°. The values obtained are higher when compared to the work of Dankovich and Gray[16] when they investigated the contact angle of smooth nanocrystalline cellulose (I) and regenerated samples. The only difference was that they prepared a thin film layer from their CNC samples. It should be noted that the regenerated

CNC sample was obtained by caustic treatment in this study and in that by Dankovich and Gray.[16] In the end, the values obtained in this manuscript are higher than theirs because the films they prepared allowed for the sulfate and hydroxyl groups to be better exposed to water droplets. However, in our experiments, we measured the powder wettability, which depends on the amount of sample packed as well as the efficiency of packing.

The contact angle of the CNC_SD sample is significantly lower than the contact angles reported for the CNC_Std sample only. In the other cases, it is within the range of the CNC_FD and CNC_Reg samples. A plausible reason for this is the better reproducibility among values for the CNC_Std samples, which may have arisen from this sample being better purified.

In summary, the polarities of the different samples, in most cases, are not significantly different at $p < 0.05$. Despite the removal of impurities to the acid hydrolysis, during the production of CNC_Reg, there was no clear demarcation in properties.

X-ray photoelectron spectroscopy characterization

XPS was used to survey the abundance of different carbon functionalities. The signatures examined were C-C (285 eV), C-C-O (286.1-286.6), and O-C-O (288 eV).[17] The results for the different samples are presented in Table 2. Notably, the integration peak for –COOH was absent in the samples analyzed. One plausible reason for this might be the high concentration of sulfate ester bonds, as evident from the relatively high concentration of sulfur (S). In fact, the concentration of S 2p was significantly higher than that reported by Zoppe, Johansson and Seppala.[18]

Careful observation of the samples reveals that the regenerated CNC is very similar to the standard CNC sample. Given that the dissolving pulp was pretreated with caustic, the trace amounts (<10%) of hemicellulose and lignin might have been removed. As a result, the sample was more concentrated in cellulose prior to acid treatment. The interferences caused by impurities were avoided with this processing stage.

CNC_Std and CNC_Reg were characterized with low O/C ratios, indicating a significant reduction in oxygen species when compared to carbon rich species. One plausible reason for this might be because CNC_Std was prepared from cotton linters (a highly pure source), while the CNC_Reg sample was void of any substantial hemicellulosic impurities, which can adversely affect the quality of the CNC produced.

Table 1
Contact angle of CNC samples

Sample	Label	Contact angle (°)
Standard	CNC_Std	44.1 ± 0.39
Freeze dried	CNC_FD	43.7 ± 2.32
Spray dried	CNC_SD	39.1 ± 2.81
Regenerated	CNC_Reg	43.3 ± 1.39

Table 2
Abundance of different C1s signatures, O/C ratio and S content

Sample	Abundance of C1s fractions			O/C	[S]
	C-C	C-C-O	O-C-O		
CNC_Std	20.1 ± 1.34[a]	57.3 ± 1.92[b]	18.2 ± 2.12[a]	0.73 ± 0.01[b]	0.58 ± 0.02[a]
CNC_FD	9.75 ± 3.72[b]	71.5 ± 2.04[a]	19.0 ± 2.78[a]	0.90 ± 0.05[a]	0.52 ± 0.04[a]
CNC_SD	18.2 ± 2.94[a]	71.1 ± 5.67[a]	10.8 ± 2.75[b]	0.82 ± 0.01[a]	0.52 ± 0.01[a]
CNC_Reg	23.4 ± 4.68[a]	59.2 ± 3.71[b]	17.4 ± 1.15[a]	0.75 ± 0.04[b]	0.57 ± 0.01[a]

[a-b] Fractions with different letters are significantly different at $p < 0.05$

Finally, the percentage of S was higher (though not significant) for the CNC_Std and CNC_Reg samples because the feedstock for CNC production in both cases was of higher purity, allowing for better acid penetration, facilitating uniform distribution of sulfate ester

bonds on the surface. In summary, XPS was used to confirm that physical processing (drying) does not interfere with the chemical signatures.

Infrared spectroscopy characterization

Fourier transform infrared spectroscopy was used to investigate the chemical fingerprints of the different CNC samples. The different spectrum for each sample is shown in Figure 1. The peaks present in all the samples at approximately 3300-3400 and 2850-2900 cm^{-1} are due to -O-H stretching of cellulose and -C-H stretching, respectively.[19]

Upon a closer look at Figure 1, several of the peaks characteristic of CNC, as reported by Normand, Moriana and Ek,[19] are visible. The peak at 1000 and 1250 cm^{-1} represents -C-O stretching. There are marked reductions in the intensity of these two peaks for CNC_Reg. The reason for this is not clear at the moment, but one plausible reason might be a better distribution of the sulfur ester surface coverage.

Costa[20] *et al*. reported similar IR spectra when they extracted and characterized CNCs from corn stover. Interestingly, the relative size of the peak at approximately 3400 cm^{-1} for their sample characterization was larger. As mentioned earlier, this peak is due to the –O-H stretch in adsorbed water in samples. Also, the relatively smaller intensity of the peak at 1647 cm^{-1}, attributed to the –OH bending of absorbed moisture in the cellulosic network, confirmed the samples were void of moisture. Hence, it can be appreciated that the samples in our study were more effectively dried. Also, careful observation of Figure 3 reveals a peak at 1375 cm^{-1} for all the samples. Costa[20] *et al*. reported that this peak is due to the C-H vibration during the asymmetric deformation of cellulose. Despite the drying technologies, Moran[21] *et al*. reported that the O-H signatures would always be present because of the strong cellulose-water interaction.

In summary, IR spectroscopy is a qualitative technique used to decipher the chemical functionalities associated with a chemical system. In this case, there are minute differences among the different CNC samples, but not large enough to highlight. In the end, the signatures of interest highlighted previously are present in all the samples.

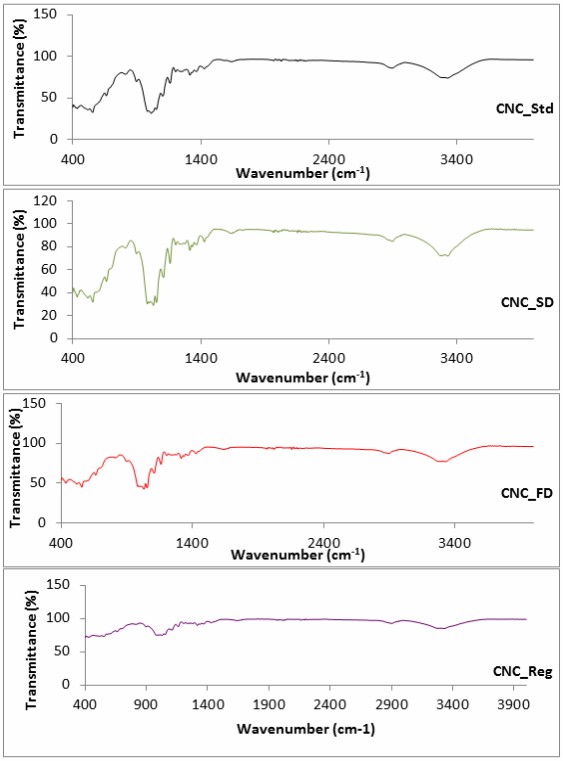

Figure 1: IR spectra of different CNC samples, range 400 to 4000 cm^{-1}

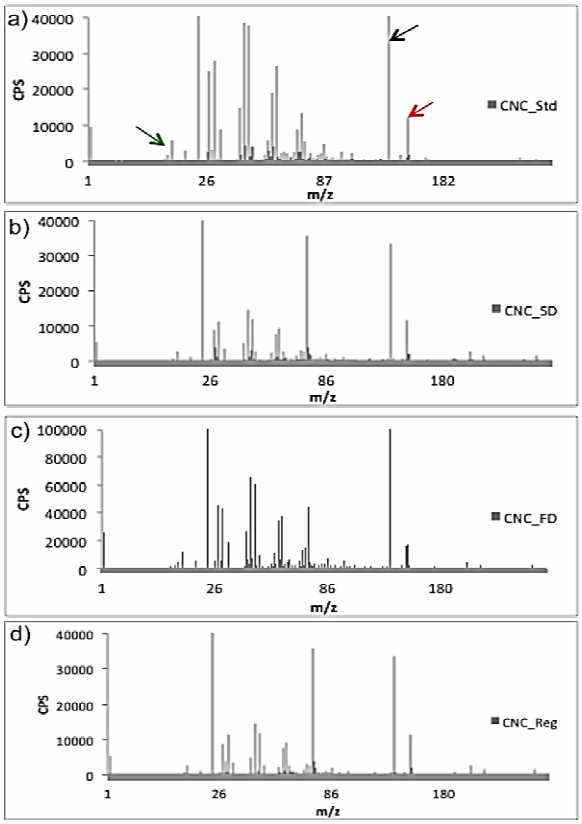

Figure 2: ToF-SIMS spectra of a) CNC_Std, b) CNC_SD, c) CNC_FD, and d) CNC_Reg sample

Time of flight secondary ion mass spectroscopy (ToF-SIMS) characterization

The surfaces of the different CNC samples were characterized using secondary ion mass spectroscopy. The main aim was to determine whether there are intact cellulosic peaks after acid hydrolysis. Figure 2 shows the positive ion mass spectra (m/z 0-250) obtained from the various CNC samples. Characteristic SIMS ion fragments of cellulosic were identified according to published literature values.[22-23] All the CNC samples were characterized with the two dominant peaks for cellulose at 127 (black arrow) and 145 (red arrow) corresponding to m/z for ($C_6H_7O_3^+$) and ($C_6H_9O_4^+$), respectively. Interestingly, all the spectra were characterized with a Na^+ peak at approximately 23 m/z (green arrow). It is well known that sodium ions balance the charge of the hydroxyl, carboxyl and sulfate ester groups of the CNC samples.[1,24]

The different fractions below 80 m/z are predominantly due to the cleavage of the cellulosic network producing $C_3H_4^+$ (40 m/z), $C_2H_5O^+$ (45 m/z), and $C_5H_{11}^+$ (71 m/z).[25]

In summary, given that the samples are chemically similar, much difference was not observed among the samples. In fact, the peaks characteristic of cellulose were the dominant peaks and the fragments present in the spectra were from fragmentation of cellulose.

Thermal properties

The thermal stability of the different CNC samples was evaluated using thermal gravimetric analysis. The different parameters are presented in Table 3. The thermographs for the different samples were characterized with two main stability peaks, denoted as T_{max} for the two processes. Also, the initial temperature of degradation was calculated and reported as T_o. The initial degradation temperature is the first observed significant decrease in stability of the samples with increased heating.

Interestingly, for the first process and second process, the temperature ranges that were observed were within ranges of 290-310 and 360-370 °C, respectively. This points to little difference among the samples on a bulk scale. In addition, the CNC_Std and CNC_Reg were characterized with better or higher initial

degradation temperatures. Plausible reasons for this may be the absence of surface defects within the particles that may have resulted from the pretreatment or lack of lignin/hemicellulosic impurities. Finally, both these samples were characterized with significantly ($p<0.05$) lower ash content when compared to the CNC_SD or CNC_FD samples. Again, the lack of impurities may have contributed to this.

In summary, little difference was observed among the different CNC samples studied, but the CNC_Std and CNC_Reg are better for high temperature applications due to their superior initial degradation temperatures.

Finally, Costa[20] *et al*. reported similar numbers for T_{max}. In fact, they reported a temperature of 302 °C for the first degradation stage. Interestingly, their samples were void of the second T_{max} observed in this study. Also, they echoed the same observation that the introduction of the ($O\text{-}SO_3H$) groups onto the surface significantly reduces the thermal resistance of the particles.

Bulk properties

Crystallinity data

The crystallinity index (CI) of the different CNC samples was investigated using X-ray diffraction methodology. A method developed at National Research Council of Canada based in the National Institute of Nanotechnology was used to estimate the index for the different samples. The method involved fitting the spectra obtained using the software outlined in the methodology section and then using a calibration curve with different types of CNC obtained from different feedstock sources to estimate the CI. The CI for the different samples is presented in Table 4.

Also, the crystallinity was studied because it has implications on the physical, mechanical, and chemical properties of cellulose-based materials. For instance, with increasing CI, there is a corresponding increase in tensile strength, dimensional stability, and density. On the other hand, material properties, such as reactivity and swelling, decrease accordingly.[26-27] A representation of the different diffractograms is presented in Figure 3. It should be noted, this figure just serves for the identification of the polymorph.

The method used to determine crystallinity has been a subject of great debate. Many researchers have used wide-angle X-ray diffraction[28] or Raman spectroscopy[29] to determine the crystallinity of samples. To point to this fact, consider the value obtained when the researchers at NRC characterized the CNC_Std *versus* when we did it in-house at the University of Alberta. The values vary greatly and this points to the user influence on the final number. Also, the method adapted (for calibration and peak fitting) will have some influence on the final result.

Table 3
Thermal properties for different CNC samples, WL (%) – percentage weight lost at the corresponding T_{max}

Sample	T_o	First process		Second process		Ash content (%)
		T_{max}	WL (%)	T_{max}	WL (%)	
CNC_Std	247.8 ± 1.7	308.6 ± 2.7	55.1 ± 0.8	368.6 ± 6.0	14.8 ± 1.4	23.1 ± 1.3
CNC_FD	235.8 ± 0.8	289.8 ± 0.6	43.1 ± 4.2	370.3 ± 1.1	21.8 ± 16	30.0 ± 0.5
CNC_SD	237.8 ± 4.2	300.7 ± 0.6	46.3 ± 2.4	361.7 ± 8.4	20.0 ± 1.7	31.4 ± 1.7
CNC_Reg	248.6 ± 1.5	306.4 ± 1.2	52.6 ± 1.8	366.2 ± 1.2	13.5 ± 1.4	21.1 ± 1.0

Table 4
Crystallinity for different samples of CNC

Sample	Crystallinity index (%)
CNC_Std (NRC)[1]	90 ± 2.1
CNC_Std	76 ± 0.3
CNC_SD	73 ± 1.9
CNC_FD	74 ± 2.3
CNC_Reg	77 ± 0.7

[1]Values obtained from National Research Council Canada Product documentation for the Cellulose Nanocrystal Certified Reference Material

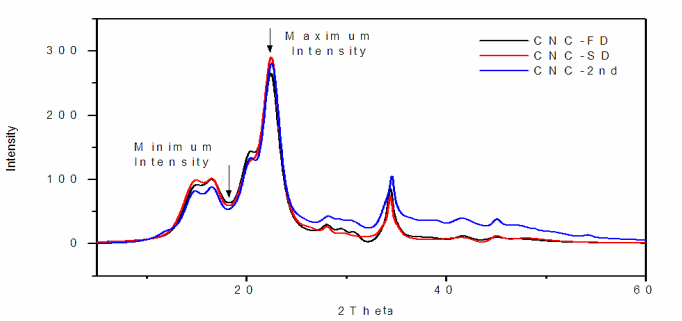

Figure 3: X-ray diffraction representation of CNC samples. Minimum intensity was measured at 2θ = 18.2°, while maximum intensity – at 2θ = 22.5°

Table 5
DLS properties of the different CNC samples

Sample	DLS			Zeta potential (mV)	pH
	Peak #	d_{av} (nm)	Int. (%)		
CNC_Std (NRC)[1]	1	95.3 ± 13.6	-	-39.3 ± 5.80	6.6
CNC_Std	1	93.2 ± 5.1	94.2 ± 5.3	-31.2 ± 0.59	6.8
	2	1149 ± 179	4.9 ± 2.2		
CNC_SD	1	123.9 ± 9.34	80.3 ± 7.31	-35.3 ± 1.03	6.9
	2	774 ± 174	10.4 ± 3.1		
	3	1723 ± 1093	4.1 ± 2.1		
CNC_FD	1	88.9 ± 3.89	91.2 ± 3.9	-31.0 ± 0.99	6.9
	2	1107 ± 105	6.1 ± .37		
CNC_Reg	1	97.1 ± 3.9	93.1 ± 3.9	-31.4 ± 1.94	6.9
	2	1134 ± 10.1	2.4 ± 2.1		

[1]Values obtained from National Research Council Canada Product documentation for the Cellulose Nanocrystal Certified Reference Material

The CI values reported in this manuscript are in agreement with those for the crystals produced from microcrystalline cellulose using ionic liquids by Man[30] *et al*. Despite the difference in feedstock and methodology used to produce the CNC, the robustness of the method is illustrated. There was no significant difference between the CI for the different samples outlined in Table 2, except when compared to the NRC CNC_Std. This is not surprising, given that the key variation between the samples was the drying method (CNC_SD *versus* CNC_FD) and a minute change in composition prior to acid hydrolysis (CNC_Reg).

Dynamic light scattering (DLS) and zeta potential measurements

The particle size and zeta potential of the different CNC samples were determined. The results for the different samples are presented in Table 5. The size distribution, percentage of the major fractions, zeta potential and pH were determined. It should be noted that the CNC samples were dispersed in water (about 2 wt%) and sonicated until good dispersion was observed. This mixture was then diluted to 0.1 wt% and mixed in a 1:1 volume with 10 mM NaCl aqueous solution to a final 0.05 wt% CNC dispersion for analysis. The suspension was finally filtered through a 0.45 µm syringe filter. The pH measurements were done using a standard electrode pH meter.

Firstly, the zeta potential of the CNC samples is a key indicator of the stability of the colloidal dispersion. In other words, the magnitude of the zeta potential indicates the degree of electrostatic repulsion between adjacent particles. According to Obrien[31] *et al*., particles within the ±30 to ±40 range are characterized with moderate stability. Thus, all the CNC samples are characterized with good stability in solution, which is an added advantage when they will eventually be used in different applications. Additionally, the samples are characterized with at least 90% particles within the 90-100 nm range. Despite these observations, it is essential to remember that the precision of DLS measurements is influenced by

the concentration of the particles in suspension, the scattering angle, and the shape anisotropy of nanoparticles.[32] Also, the samples analyzed compared well with the standard results provided by NRC. In summary, it was found that the different drying methods or pretreatment had little or no significant influence on the particle properties of the CNCs obtained.

Microscopy

Scanning electron microscopy was used to investigate the morphological distribution of the different CNC samples without re-dispersion. In other words, unlike previous publications,[33] the main aim in this communication is to identify the effects of drying on the morphological properties of the different CNC samples, as is. Dried samples of CNC studied using scanning electron microscopy are presented in Figure 4. CNC that was freeze-dried is characterized by morphology different from that of the other samples. In fact, the CNC_FD sample appeared to be a thin-layered structure that peels under the excitation rays of the SEM. On the other hand, CNC_SD, CNC_Std, and CNC_Reg were observed as definite particles with macro-dimensions. This resulted from the agglomeration of the particles during the drying process. As mentioned previously, the aim was not to re-disperse the particles, but to investigate the effect of drying on the bulk properties. Khoshkava and Kamal[34] reported similar images when they studied the effect of drying conditions on CNC agglomeration and dispersability. To that end, the same topology for freeze-dried (flaky and sheet-like) and spray dried (particles) was observed.

In summary, scanning electron microscopy can be used to investigate the effect of drying on the morphological features of CNC. CNC_Std was similar to CNC_Reg based on preliminary images presented.

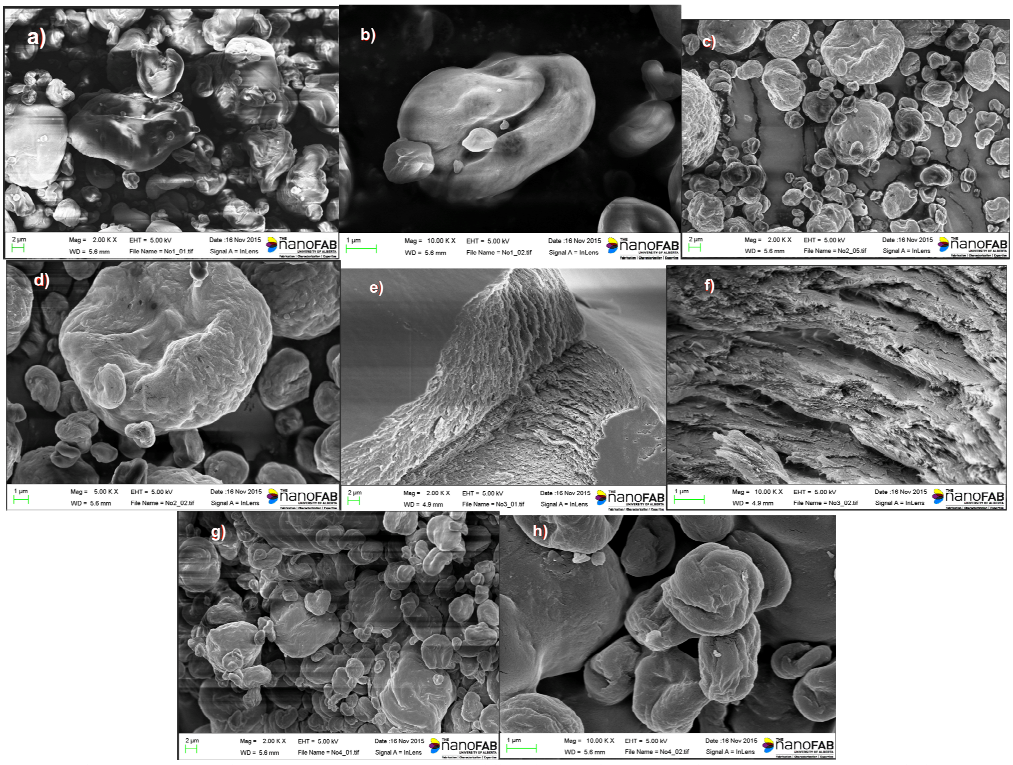

Figure 4: Scanning electron micrographs taken at magnifications of 2000 (left pane) and 10000 (right pane) for a-b) CNC_Std, c-d) CNC_SD, e-f) CNC_FD, and g-h) CNC_Reg

CONCLUSION

This study highlighted that spray drying and freeze-drying of CNC particles result in their intricate features that can be application specific. The two techniques force distinct changes in the morphology of the CNCs. In other words, there are distinct agglomeration mechanisms occurring among the CNC particles during each drying method. On the other hand, there is little to differentiate between the two methods with respect to the surface and bulk properties. Further, pretreating the pulp material with a caustic

solution prior to acid digestion resulted in a material that had comparable properties to that of the standard supplied by National Research Council Canada. In the end, the method selected to dry CNCs prior to shipping/transport or for specific applications, will depend on the cost of scaling the equipment and the desired properties.

ACKNOWLEDGEMENTS: The authors acknowledge the Government of Alberta for the financial support. The authors are grateful to Alberta Innovates Technology Futures (AITF) for kindly supplying the CNC samples needed for this study. Also, the authors are thankful to Dr. Christophe Danumah for supplying the standard sample.

REFERENCES

[1] Y. Habibi, L. A. Lucia and O. J. Rojas, *Chem. Rev.*, **110**, 3479 (2010).
[2] B. G. Ranby, *Acta Chem. Scand.*, **3**, 649 (1949).
[3] B. G. Ranby and E. Ribi, *Experientia*, **6**, 12 (1950).
[4] K. Benhamou, H. Kaddami, A. Magnin, A. Dufresne and A. Ahmad, *Carbohyd. Polym.*, **122**, 202 (2015).
[5] A. Sutka, J. Gravitis, S. Kukle, A. Sutka and M. Timusk, *Soft Mater.*, **13**, 18 (2015).
[6] J. O. Shatkin, T. H. Wegner, E. M. Bilek and J. Cowie, *TAPPI J.*, **13**, 9 (2014).
[7] S. Beck, J. Bouchard and R. Berry, *Biomacromolecules*, **13**, 1486 (2012).
[8] Y. Peng, D. J. Gardner and Y. Han, *Cellulose*, **19**, 91 (2012).
[9] M. George, P. Mussone and D. Bressler, *J. Wood Chem. Technol.*, **3**, 114 (2015).
[10] M. George, P. Mussone and D. Bressler, *Ind. Crop. Prod.*, **53**, 365 (2014).
[11] H. Sehaqui, N. E. Mushi, S. Morimune, M. Salajkova, T. Nishino *et al.*, *ACS Appl. Mater. Interf.*, **4**, 1043 (2012).
[12] S. Park, J. O. Baker, M. E. Himmel, P. A. Parilla and D. K. Johnson, *Biotechnol. Biofuels*, **3**, 10 (2010).
[13] A. Kumar, Y. S. Negi, V. Choudhary and N. K. Bhardwaj, *J. Mater. Phys. Chem.*, **2**, 1 (2014).
[14] Q. Lu, X. Hu, X. Wang, J. A. Kluge, S. Lu *et al.*, *Acta Biomater.*, **6**, 1380 (2010).
[15] P. Lu and Y. Hsieh, *Carbohyd. Polym.*, **82**, 329 (2010).
[16] T. A. Dankovich and D. G. Gray, *J. Adhes. Sci. Technol.*, **25**, 699 (2011).
[17] A. P. Mathew, K. Oksman, Z. Karim, P. Liu, S. A. Khan *et al.*, *Ind. Crop. Prod.*, **58**, 212 (2014).
[18] J. O. Zoppe, L. Johansson and J. Seppälä, *Carbohyd. Polym.*, **126**, 23 (2015).
[19] M. Le Normand, R. Moriana and M. Ek, *Carbohyd. Polym.*, **111**, 979 (2014).
[20] L. A. D. S. Costa, A. F. Fonseca, F. V. Pereira and J. I. Druzian, *Cellulose Chem. Technol.*, **49**, 127 (2015).
[21] J. I. Moran, V. A. Alvarez, V. P. Cyras and A. Vazquez, *Cellulose*, **15**, 149 (2008).
[22] S. Jung, M. Foston, M. C. Sullards and A. J. Ragauskas, *Energ. Fuel.*, **24**, 1347 (2010).
[23] N. E. Zafeiropoulos, D. R. Williams, C. A. Baillie and F. L. Matthews, *Composites Part A*, **33**, 1083 (2002).
[24] N. Duran, A. P. Lemes and A. B. Seabra, *Recent Pat. Nanotech.*, **6**, 16 (2012).
[25] Y. Deslandes, G. Pleizier, E. Poire, S. Sapieha, M. Wertheimer *et al.*, *Plasmas Polym.*, **3**, 61 (1998).
[26] J. Lamaming, R. Hashim, C. P. Leh, O. Sulaiman, T. Sugimoto *et al.*, *Carbohyd. Polym.*, **134**, 534 (2015).
[27] L. P. Novo, J. Bras, A. Garcia, N. Belgacem and A. A. S. Curvelo, *ACS Sustain. Chem. Eng.*, **3**, 2839 (2015).
[28] J. Balko, R. H. Lohwasser, M. Sommer, M. Thelakkat and T. Thurn-Albrecht, *Macromolecules*, **46**, 9642 (2013).
[29] A. L. Weisman, K. H. DuBay, K. A. Willets and R. A. Friesner, *J. Chem. Phys.*, **141**, 224702 (2014).
[30] Z. Man, N. Muhammad, A. Sarwono, M. A. Bustam, M. V. Kumar *et al.*, *J. Polym. Environ.*, **19**, 726 (2011).
[31] R. W. Obrien, B. R. Midmore, A. Lamb and R. J. Hunter, *Faraday Discuss.*, **90**, 301 (1990).
[32] K. Takahashi, H. Kato, T. Saito, S. Matsuyama and S. Kinugasa, *Part. Part. Syst. Char.*, **25**, 31 (2008).
[33] J. Han, C. Zhou, Y. Wu, F. Liu and Wu, Q. *Biomacromolecules*, **14**, 1529 (2013).
[34] V. Khoshkava and M. R. Kamal, *Powder Technol.*, **261**, 288 (2014).